

Kinetic modeling of hydrogen production by the catalytic reforming of crude ethanol over a co-precipitated Ni-Al₂O₃ catalyst in a packed bed tubular reactor

Abayomi Akande^{a, c}, Ahmed Aboudheir^b, Raphael Idem^{a, *}, Ajay Dalai^c

^aProcess Systems Engineering Laboratory, Faculty of Engineering, University of Regina, Regina, SK, Canada S4S 0A2

^bHTC Hydrogen Thermochem Corp, Regina, SK, Canada S4P 0S7

^cDepartment of Chemical Engineering, University of Saskatchewan, Saskatoon, SK, Canada S7N 5C5

Available online 20 February 2006

Abstract

In this work, we performed a kinetic modeling of the production of hydrogen by the catalytic reforming of crude ethanol over a 15%-Ni/Al₂O₃ catalyst prepared by the co-precipitation technique. The kinetics experiments were carried out at atmospheric pressure in a packed bed tubular reactor (8 mm inside diameter, 150 mm heated length, 53.0 mm bed height), at temperature in the range of 593–793 K. Eley Rideal assumptions where the surface reaction involved an adsorbed species and a free gaseous species were used to develop the reaction mechanism and four models were proposed based on this mechanism, from which a new kinetic model based on the dissociation of adsorbed crude ethanol as the rate-determining step was developed for this novel catalytic process. This model was of the form: $-r_A = (2.08 \times 10^3 e^{-4430/RT} N_A) / [1 + 3.83 \times 10^7 N_A]^2$. The absolute average deviation between experimental rates and those predicted using this model was 6%.

© 2006 International Association for Hydrogen Energy. Published by Elsevier Ltd. All rights reserved.

Keywords: Crude ethanol; Catalytic reforming; Hydrogen production; Kinetic modeling

1. Introduction

The demand for hydrogen energy has increased tremendously in recent years essentially because of the increase in the world energy consumption as well as the recent developments in fuel cell technologies. The Energy Information Administration has projected that world energy consumption will increase by 59% over the next two decades, and the largest share will still be dominated by fossil fuels. Carbon dioxide (CO₂)

emissions resulting from the combustion of fossil fuels currently are estimated to account for three-fourths of human-caused CO₂ emissions worldwide. Greenhouse gas emissions, including CO₂, should be limited, as recommended at the Kyoto Conference, Japan, in December 1997. In this regard, hydrogen (H₂) has a significant future potential as an alternative fuel that can solve the problems of CO₂ emissions. One of the techniques to produce hydrogen is by steam reforming of hydrocarbons or biomass. Crude ethanol (i.e. fermentation broth) is a form of biomass, which is easy to produce, free of sulfur, has low toxicity, and is also safe to handle, transport and store. All the oxygenated hydrocarbons in crude ethanol can be reformed completely to H₂ and CO₂, the latter of which could be separated from H₂ by

* Corresponding author. Tel.: +1 306 585 4470;

fax: +1 306 585 4855.

E-mail address: raphael.idem@uregina.ca (R. Idem).

Nomenclature

C_i	concentration of species i , kmol/m ³	L	height of catalyst bed, mm
D_p	catalyst particle diameter, mm	r_A	rate of crude-ethanol conversion, kmol crude/kg cat s
(a)	active sites	RDS	rate-determining step
D	internal diameter of reactor, mm	W	weight of catalyst, kg
E	activation energy, kJ/kmol	X	crude-ethanol conversion mol% or fractional conversion
k_0	collision frequency or pre-exponential constant, (kg cat s) ⁻¹	AAD%	average absolute deviation, %
K_i	equilibrium constant of reaction step i	W/F_{A0}	space time, kg cat s/kg crude
K_p	overall equilibrium constant	N_i	molar flow rate of species kmol/s
R	universal gas constant, kJ/kmol K		

membrane technology. This provides for CO₂ capture for eventual storage or destruction, thereby resulting in negative CO₂ emissions [1–12].

The production of hydrogen by steam reforming of pure ethanol has been widely investigated. Jordi et al. [13] investigated the effect of Co/ZnO catalyst on ethanol reforming, using a high water to ethanol molar ratio of 13:1 (20% v/v ethanol) as their reaction mixture. They reported complete ethanol conversion of 100%, high H₂ selectivity of 66% and CO₂ selectivity of 20.8% in the reaction products. Also, Leclerc et al. [14] reported that hydrogen yield and ethanol conversion were influenced by increase in water to ethanol ratio. Ethanol conversion close to 100% and hydrogen yield of 5.56 mols per mol of ethanol reacted were obtained at water to ethanol molar ratio of 20:1 and temperature between 798 and 1198 K. In addition, the high water to ethanol ratio inhibited the production of undesirable product such as methane (CH₄), carbon monoxide (CO), acetaldehyde, ethylene and carbon. Gavita et al. [15] investigated the effects of Ni/MgO catalyst on steam reforming of ethanol using water to ethanol molar ratios of 1.04:1 and 8.1:1. They reported that in both cases the ethanol conversion and the concentration of H₂, CO₂ and CH₄ increased with temperature. The conversion reached 100% at temperatures above 573 K. Das [16] investigated the ethanol steam reforming reaction on Mn promoted Cu/Al₂O₃ catalyst at water to ethanol molar ratios of 3:1–15:1. He reported that ethanol conversion increased with an increase in water to ethanol molar ratio. An optimum water to ethanol molar ratio of 6:1 (35% v/v ethanol) was observed with an ethanol conversion of 50% after which there was no significant increase in conversion.

In all these cases, water is needed as a co-feed to the process. Consequently, there is no need to reduce the water and organic contents of wet or crude ethanol (i.e.

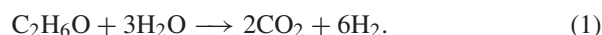
fermentation broth produced from a fermentation process) since this contains approximately 12% v/v ethanol, which is within the range of water to ethanol molar ratios used in literature cited ethanol reforming processes. Besides, by using crude ethanol, the other organic compounds present in the fermentation broth could equally be reformed to produce additional H₂. Also, this process would eliminate the large amount of energy wasted during distillation to remove water from fermentation broth in order to produce dry or pure ethanol. It was suggested by Haga et al. [2] that in order to obtain a widespread use of ethanol for hydrogen production, the economics and energetics of the ethanol production process have to be greatly improved. Thus, by circumventing the distillation and drying step, our process [17,18] of reforming crude ethanol (i.e. fermentation broth) provides us with the ability to produce H₂ from crude ethanol solution in a cost-effective manner. However, the reforming of crude ethanol to produce hydrogen has not been reported in the literature before, to the best of our knowledge, until we recently developed the catalytic process for H₂ production from the reforming of crude ethanol based on Cu/Mn/Al₂O₃ and Ni/Al₂O₃ catalysts [17,18].

It is well known that the simulation and design of any reactor requires information on both the thermodynamic and kinetic properties of the reaction of interest. While there is little information on both properties regarding the steam reforming of pure ethanol, there is no such information in the case of the reforming of crude ethanol. In our earlier work reported elsewhere [18], we examined the activities of a large number of Ni/Al₂O₃ catalysts. The results showed that the catalyst with 15 wt% Ni loading on alumina support that was prepared by coprecipitation was the optimum catalyst and gave a maximum conversion of crude ethanol of 79% on a molar basis at 673 K and W/F_{A0} of 2143 kg cat s/kg crude

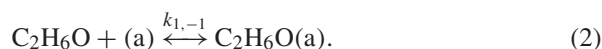
ethanol. In the present work, we have performed the kinetic modeling of H₂ production by the reforming of crude ethanol using this catalyst. The overall objective was to obtain an intrinsic rate equation using methods of experimentation and analysis, which are based on fundamental kinetics studies. The derivation of this rate equation was based on the mechanistic description of the crude ethanol reforming process together with extensive kinetic measurements. An attempt was also made to fit the experimental data to a power law rate model. The results of these derivations, measurements and analyses are presented and discussed in this paper.

2. Kinetic modeling

Ethanol reforming reaction can be represented by Eq. (1)



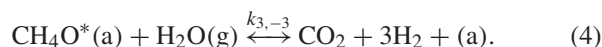
Three basic steps based on Eley Rideal mechanism were used in the derivation of the mechanistic type rate equations with the assumption that intrinsic data were collected, and as such, mass and heat transfer limitations were absent. In this mechanism, step one is the adsorption of crude ethanol on the catalyst surface; step two is the interaction of the adsorbed crude ethanol with an adjacent vacant site while step three involves two types of surface reactions between an adsorbed species and an unadsorbed species in the gaseous state. The mechanism is as given in Eqs. (2)–(5) using the chemical formula for ethanol for simplicity. Adsorption of crude ethanol on an active site:



Dissociation of adsorbed crude ethanol into hydrocarbon and oxygenated hydrocarbon fractions:



Surface reaction of adsorbed oxygenated hydrocarbon fraction with non-adsorbed water vapor:

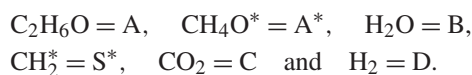


Surface reaction of adsorbed hydrocarbon fraction with non-adsorbed water vapor:



where (a) represents an active site, k_i represents the forward reaction rate constant for reaction i , and k_{-i} represents the backward reaction rate constant for reaction i .

Let



We are evaluating four cases as possible rate controlling mechanisms for the catalytic reforming of crude ethanol over coprecipitated Ni/Al₂O₃ catalyst. In the first case (i.e. formulation of model #1), adsorption of crude ethanol (Eq. (2)), is assumed as the rate-determining step (RDS).

This resulted in the rate model as given in the following equation:

$$r_A = \frac{k_0 e^{-E/RT} [C_A - (C_C^2 C_D^6 / K_P C_B^3)]}{[1 + (K_F C_C C_D^3 / C_B) + (K_G C_C C_D^3 / C_B^2) + (K_E C_C^2 C_D^6 / C_B^3)]}. \quad (6)$$

In the second case (formulation of model #2), Eq. (3), the dissociation of adsorbed crude ethanol (which requires an additional active site) is assumed as the RDS. This resulted in rate model as given below

$$r_A = \frac{k_0 e^{-E/RT} (C_A - (C_C^2 C_D^6 / K_P C_B^3))}{[1 + K_A C_A + (K_F C_C C_D^3 / C_B) + (K_G C_C C_D^3 / C_B^2)]^2}. \quad (7)$$

In the third case (for formulation of model # 3), surface reaction 4 is assumed to be the RDS. This resulted in rate model as given below

$$r_A = \frac{k_0 e^{-E/RT} ((C_A C_B^3 / C_C C_D^3) - (C_C C_D^3 / K_P))}{(1 + K_A C_A + (K_Q C_A C_B^3 / C_C C_D^3) + (K_G C_C C_D^3 / C_B^2))}. \quad (8)$$

The fourth case (for formulation of model #4) involved the assumption of surface reaction 5 as the RDS. This resulted in rate model as given below

$$r_A = \frac{k_0 e^{-E/RT} ((C_A C_B^3 / C_C C_D^3) - (C_C C_D^3 / K_P))}{(1 + K_A C_A + (K_F C_C C_D^3 / C_B) + (K_H C_A C_B / C_C C_D^3))}. \quad (9)$$

Finally, the power law model was also used to fit the experimental data. The model is of the form

$$r_A = k_0 e^{-E/RT} C_A^n, \quad (10)$$

where n , is the order of reaction with respect to crude ethanol. This form of the power law model (i.e. no terms involving the concentrations of H₂O and the products, H₂ and CO₂) was adopted because H₂O was present in a large excess as compared to the combined concentration of the organic components of the crude, C_A, and because the reaction was more or less irreversible within the temperature range used in the kinetic studies. These models are all summarized in Table 1 in terms of concentration of species and the species molar flow rates.

Table 1
Table of kinetic models

RDS	Models based on species concentration	Models based on species molar flow
Adsorption of crude ethanol	$r_A = \frac{k_0 e^{-E/RT} \left[C_A - \frac{C_C^2 C_D^6}{K_P C_B^3} \right]}{\left[1 + \frac{K_F C_C C_D^3}{C_B} + \frac{K_G C_C C_D^3}{C_B^2} + \frac{K_E C_C^2 C_D^6}{C_B^3} \right]}$	$r_A = \frac{k_0 e^{-E/RT} \left[N_A - \frac{N_C^2 N_D^6}{K_P N_B^3} \right]}{\left[1 + \frac{K_F N_C N_D^3}{N_B} + \frac{K_G N_C N_D^3}{N_B^2} + \frac{K_E N_C^2 N_D^6}{N_B^3} \right]}$
The dissociation of adsorbed crude ethanol	$r_A = \frac{k_0 e^{-E/RT} \left(C_A - \frac{C_C^2 C_D^6}{K_P C_B^3} \right)}{\left[1 + K_A C_A + \frac{K_F C_C C_D^3}{C_B} + \frac{K_G C_C C_D^3}{C_B^2} \right]^2}$	$r_A = \frac{k_0 e^{-E/RT} \left(N_A - \frac{N_C^2 N_D^6}{K_P N_B^3} \right)}{\left[1 + K_A N_A + \frac{K_F N_C N_D^3}{N_B} + \frac{K_G N_C N_D^3}{N_B^2} \right]^2}$
Surface reaction between adsorbed oxygenated hydrocarbon and steam	$r_A = \frac{k_0 e^{-E/RT} \left(\frac{C_A C_B^3}{C_C C_D^3} - \frac{C_C C_D^3}{K_P} \right)}{\left(1 + K_A C_A + \frac{K_Q C_A C_B^2}{C_C C_D^3} + \frac{K_G C_C C_D^3}{C_B^2} \right)}$	$r_A = \frac{k_0 e^{-E/RT} \left(\frac{N_A N_B^3}{N_C N_D^3} - \frac{N_C N_D^3}{K_P} \right)}{\left(1 + K_A N_A + \frac{K_Q N_A N_B^2}{N_C N_D^3} + \frac{K_G N_C N_D^3}{N_B^2} \right)}$
Surface reaction between adsorbed s hydrocarbon fraction species and steam	$r_A = \frac{k_0 e^{-E/RT} \left(\frac{C_A C_B^3}{C_C C_D^3} - \frac{C_C C_D^3}{K_P} \right)}{\left(1 + K_A C_A + \frac{K_F C_C C_D^3}{C_B} + \frac{K_H C_A C_B}{C_C C_D^3} \right)}$	$r_A = \frac{k_0 e^{-E/RT} \left(\frac{N_A N_B^3}{N_C N_D^3} - \frac{N_C N_D^3}{K_P} \right)}{\left(1 + K_A N_A + \frac{K_F N_C N_D^3}{N_B} + \frac{K_H N_A N_B}{N_C N_D^3} \right)}$

3. Experimental details

3.1. Crude ethanol

The crude ethanol (i.e. fermentation broth) used for this work was obtained from Pound Maker Agventures, Lanigan, Saskatchewan, Canada. In this work, crude ethanol is defined as the combination of all the oxygenated hydrocarbon components of fermentation broth; namely, ethanol, lactic acid, glycerol and maltose. We performed an analysis in our laboratory to both identify and quantify these components of fermentation broth using a high performance liquid chromatograph (HPLC) model Agilent 1100 series supplied by Agilent Technologies, Wilmington, Delaware, USA. The HPLC was equipped with a 250 by 4.1 mm HC-75 column and a refractive index detector, while 0.05 mM succinic acid was used as the mobile phase. The result of the analysis is shown in Table 2. Consequently, the overall molecular formula of crude ethanol based on the weighted average of these components is $C_{2.12}H_{6.12}O_{1.23}$. Based on this composition, the general equation representing the reforming of crude ethanol can be represented as

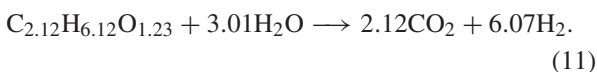


Table 2
Crude ethanol composition

Crude ethanol components	Volume%	Mole % on a water free basis
Ethanol	12.0	88.42
Lactic acid	1.0	5.71
Glycerol	1.0	5.87
Maltose	0.001	0.001
Water	86.0	Not applicable

However, for the sake of simplicity, and because the stoichiometry of ethanol steam reforming is well known and more familiar, it was used to develop the kinetics. There was no loss of accuracy by doing this since the atomic ratios indicated in Eq. (1) were used just as illustrations of the presence of carbon, hydrogen and oxygen atoms in the organic fraction of the feed but not for any calculations. Also, the error incurred in using an average formula instead of the formulas of individual components was less than 7% based on the contributions of the other organic materials in the reaction mixture.

3.2. Catalyst

The catalyst used in this work was a 15% Ni/Al₂O₃ catalyst. This catalyst had a BET surface area of

81 m²/g, average pore size of 145 Å, and pore volume of 0.29 cm³/g. The species present in the catalyst based on powder X-ray diffraction (XRD) analysis were NiO, Al₂O₃ and NiAl₂O₄. X-ray line broadening calculations gave a value of 29.8 nm as the crystallite size of NiO on the catalyst. Details concerning the preparation as well as the physico-chemical characteristics of this catalyst are given elsewhere [18].

3.3. Kinetic studies

Kinetic data for H₂ production by the reforming of crude ethanol reforming process were obtained using a conventional fixed bed reactor operated isothermally at atmospheric pressure. The reactor used to obtain kinetic data was BTRS model number 02250192-1 supplied by Autoclave Engineers, Erie, PA, USA. It was made of a stainless steel tube of 8 mm internal diameter placed in an electric furnace. Crude ethanol was supplied to the reactor chamber by means of a high-pressure liquid chromatography (HPLC) pump regulated at the desired flow rates. The reaction temperature was measured with a sliding thermocouple placed inside the bed with an accuracy of ±1 K of readings.

A typical run for the reforming of crude ethanol was performed as follows: approximately 1 g of the catalyst was mixed with 2 g of pyrex glass (inert material) of the same average particle size and then loaded into the reactor. The feed consisting of crude ethanol (comprising of ethanol plus other organics and water) was then pumped at the desired flow rate to the vaporizer maintained at 523 K before entering the reactor. Prior to reaction the catalyst was reduced in situ by treatment with 5% H₂/N₂ gas (supplied by PRAXAIR, Regina, SK, Canada) flowing at 1.67 × 10⁻⁶ m³/s for 2 h. The reactions were carried out at atmospheric pressure and temperatures in the range of 593–793 K. The product mixture during reaction was passed through a condenser and gas–liquid separator to separate the gaseous and liquid products for analysis.

3.4. Product analysis

The liquid product was analyzed using the same HPLC technique described earlier. The liquid product was also analyzed using a gas chromatograph-mass spectrometer (GC-MS) technique in order to identify the components for subsequent HPLC analysis. GC-MS analysis was performed using GC-MS model HP 6890/5073 supplied by Hewlett-Packard, Quebec, Canada. An HP-Innowax column (length = 30 m, internal diameter = 250 μm, thickness = 0.25 μm) packed

with cross-linked-poly-ethylene glycol was used in the GC for the separation of components. The composition of the reformer product gas stream was analyzed on-line by gas chromatography (Model HP 6890) using molecular sieve and Haysep columns, and a thermal conductivity detector (TCD) with helium as the carrier gas. The schematic diagram of the experimental setup used for obtaining kinetic data is shown in Fig. 1.

3.5. Kinetic data

The experiments to collect kinetic data were conducted in a catalyst bed such that fluids channeling and back mixing were absent. These conditions were achieved by employing catalyst in the appropriate average size range, appropriate feed space velocity, and residence time as well as other conditions necessary and required for plug flow and isothermal behavior in the reactor. These conditions were experimentally determined using the procedure described by Idem and Bakhshi [19].

The experiments to collect the intrinsic kinetic data were eventually performed at reaction temperatures of 593, 693 and 793 K, and ratios of weight of catalyst to mass flow rate of crude ethanol (W/F_{A0}) of 779, 952, 1071, 1382, and 2143 kg cat s/kg crude ethanol using catalyst of 0.6 mm average particle size. According to Rase [20], Froment and Bischoff [21] and Geankoplis [22], there are other criteria for packed-bed reactors to ensure that flow conditions in the reactor are close to plug flow in order to obtain isothermal reactor operation, eliminate back mixing and minimize channeling. These are: (a) ratio of catalyst bed height to catalyst particle size (L/D_p) > 50, and (b) ratio of internal diameter of the reactor to the catalyst particle size (D/D_p) > 10. In this work L/D_p and D/D_p of 88.33 and 13.33 were, respectively, used in all kinetic experiments in order to ensure plug flow behavior in the reactor.

4. Results and discussion

4.1. Kinetic data

In this study, crude-ethanol conversion (X) was evaluated in terms of ethanol plus other organics on a water-free basis as shown in the following equation:

$$\text{Crude ethanol conversion}(X) = \frac{\text{gmol (organics) out} - \text{gmol (organics) in}}{\text{gmol (organics) in}}, \quad (12)$$

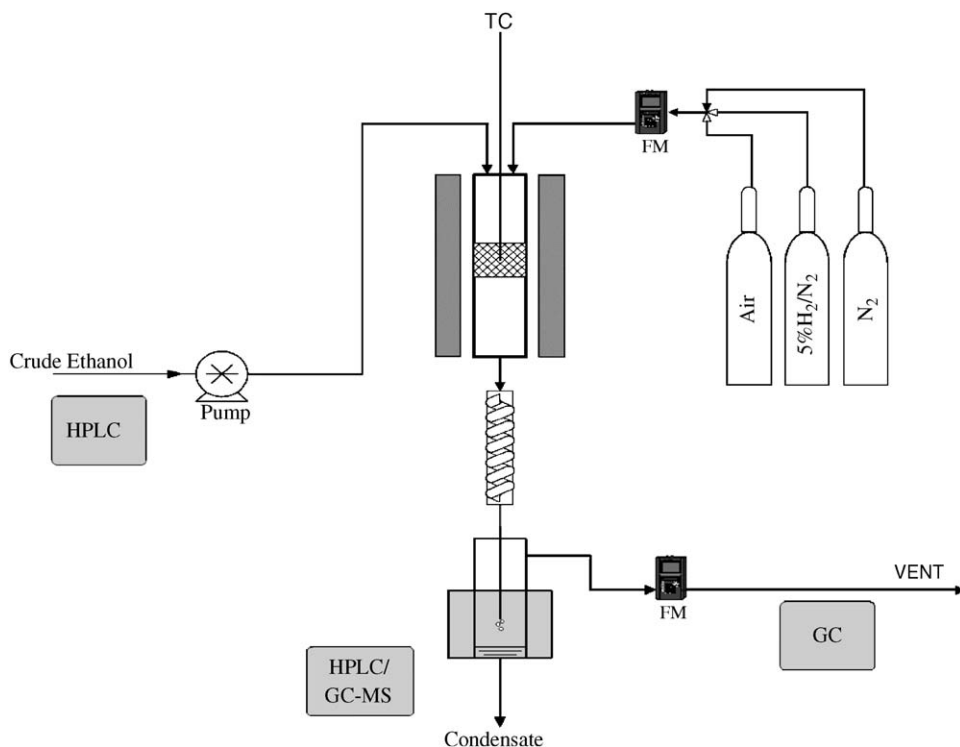


Fig. 1. Schematic diagram of the experimental setup for the catalytic packed bed tubular reactor used to obtain the kinetics data.

where organics = ethanol + lactic acid + glycerol + maltose.

Results for the variation of crude ethanol conversion (X) with ratio of weight of catalyst to crude ethanol flow rate ratio (W/F_{A0}) at reaction temperatures of 593, 693, and 793 K are presented in Fig. 2. These results show that the crude ethanol conversion initially increased rapidly with an increase in W/F_{A0} . Further increase in W/F_{A0} resulted in a slowing down of the corresponding increase of (X) for the three temperatures. These results are typical of the trend for most catalytic reactions where conversion depends on the amount of feed present.

4.2. Estimation of the parameters of rate models

A micro reactor was used to gather the experimental data and the design equation for the plug flow reactor was therefore applicable for data analysis. This was used in the differential form:

$$\frac{dX}{d(W/F_{A0})} = r_A. \quad (13)$$

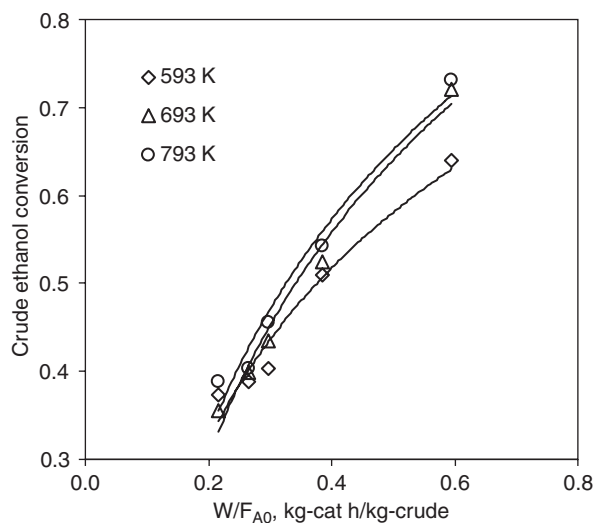


Fig. 2. Variation of crude ethanol conversion with space-time at 593, 693 and 793 K.

Slopes (i.e. $\frac{dX}{d(W/F_{A0})}$) were taken at various points of the X vs. W/F_{A0} curves within the range of the operating conditions to obtain kinetic data for the three

Table 3
Kinetics experimental data for catalytic reforming of crude ethanol

T (K)	Rate of reaction (kmol crude/kg cat s)	N_A (kmole/s)	N_B (kmole/s)	N_C (kmole/s)	N_D (kmole/s)	K_P
593	3.03286E - 06	5.70596E - 09	1.57331E - 07	8.40614E - 09	2.40685E - 08	2.45431E + 11
593	3.38489E - 06	6.96321E - 09	1.81138E - 07	8.66974E - 09	2.48233E - 08	2.45431E + 11
593	3.8669E - 06	8.43861E - 09	2.0793E - 07	8.81142E - 09	2.52289E - 08	2.45431E + 11
593	4.51138E - 06	1.03925E - 08	2.4341E - 07	8.99906E - 09	2.57662E - 08	2.45431E + 11
593	5.41583E - 06	1.64558E - 08	3.51408E - 07	9.27356E - 09	2.65521E - 08	2.45431E + 11
693	3.8669E - 06	5.02195E - 09	1.57821E - 07	1.0229E - 08	2.92878E - 08	3.36674E + 15
693	4.73885E - 06	6.94639E - 09	1.91534E - 07	1.02336E - 08	2.93008E - 08	3.36674E + 15
693	4.87424E - 06	9.80704E - 09	2.41648E - 07	1.02403E - 08	2.93201E - 08	3.36674E + 15
693	5.41583E - 06	1.27534E - 08	2.91574E - 07	1.00001E - 08	2.86323E - 08	3.36674E + 15
693	6.31485E - 06	1.73306E - 08	3.66116E - 07	9.18524E - 09	2.62993E - 08	3.36674E + 15
793	4.06187E - 06	5.11495E - 09	1.60744E - 07	1.04184E - 08	2.98302E - 08	4.45742E + 18
793	4.64136E - 06	6.56813E - 09	1.86765E - 07	1.05044E - 08	3.00763E - 08	4.45742E + 18
793	4.73885E - 06	8.52993E - 09	2.21894E - 07	1.06204E - 08	3.04085E - 08	4.45742E + 18
793	5.41583E - 06	1.20164E - 08	2.81443E - 07	1.04052E - 08	2.97921E - 08	4.45742E + 18
793	6.76978E - 06	1.62475E - 08	3.50781E - 07	9.71516E - 09	2.78165E - 08	4.45742E + 18

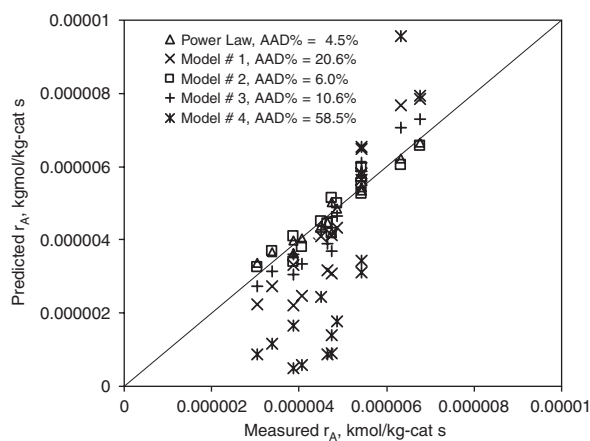


Fig. 3. A comparison of measured and predicted rates of reforming of crude ethanol within the temperature range 593–793 K and WHSV range from 4.67×10^{-4} to $1.28 \times 10^{-3} \text{ s}^{-1}$.

temperatures in order to determine experimental rates described in Eq. (13). The kinetics experimental data for catalytic reforming of crude ethanol are shown in Table 3.

The values of the parameters of the mechanism based rate models as well as the model based on power law were estimated by using a nonlinear regression procedure according to the modified Levenberg-Marquardt algorithm, which is documented in IMSL Library [23].

The subroutine called DBCLSF documented in the IMSL MATH/library [23] was used to obtain the optimum fitting parameters, because this algorithm was proven to be very efficient in estimating the mass transfer parameters, as reported elsewhere [24]. The values

obtained for the kinetics parameters are presented in Table 3.

4.3. Determination of the most realistic rate model

Fig. 3 represents the comparison of measured rates and predicted rates using rate models. A close look at this parity chart shows that models 1 and 4 did not yield satisfactory results (with average absolute deviation, AAD%, greater than 20%) whereas models 2 and 3 as well as the power law model produced satisfactory results ($\text{AAD} \leq 11\%$). In fact, model 2 in particular yielded excellent results with AAD% equal to 6%. We decided to take a closer look at both the parity chart for the rates (Fig. 3) and the estimates of the values of the parameters (Table 3) in order to elucidate the circumstances behind the behavior of each model in fitting the kinetic data. Considering the estimated values of the parameters as well as the values of the thermodynamic equilibrium constant, model 1 reduces to

$$r_A = k_0 e^{-E/RT} [N_A]. \quad (14)$$

Eq. (14) is very similar to the power law model except that the former has an order of reaction of unity whereas the power law model has an order of reaction of 0.43. Even though they both have about the same activation energies, the power law with an ADD% of 4.5% provides a better correlation of the kinetic data as compared with model 1 as shown in Fig. 3. This shows that the rate dependence of the concentration of crude ethanol was not accurately described by Eq. (14), thereby leading us to reject the assumption of the adsorption of crude

Table 4

Fitted values of kinetics constants of crude ethanol reforming to hydrogen based on the Eley Rideal rate models and the power law rate model

Parameter	Model # 1,	Model # 2,	Model # 3,	Model # 4,	Power law
K_0	8.91×10^2	2.08×10^3	1.31×10^{14}	2.75×10^{-2}	3.12×10^{-2}
E	4.03×10^3	4.43×10^3	3.55×10^3	7.56×10^3	4.41×10^3
K_A	—	3.83×10^7	1.00×10^{20}	2.27×10^{14}	—
K_E	0.0	—	—	—	—
K_F	0.0	0.0	—	1.00×10^{20}	—
K_G	0.0	0.0	0.0	—	—
K_H	—	—	—	0.0	—
K_Q	—	—	3.66×10^{12}	—	—
n	—	—	—	—	0.43
ADD	20.6%	6.0%	10.6%	58.5%	4.5%

ethanol on an active site as the rate determining mechanism for the reforming of crude ethanol. Also model # 4 had an AAD of 58.5% showing clearly that the assumed RDS was not accurate.

Also, if we now consider the estimated values of the parameters as well as the values of the thermodynamic equilibrium constant, the rate model 2 reduces to

$$r_A = \frac{k_0 e^{-E/RT} N_A}{[1 + K_A N_A]^2} \quad (15)$$

We also arrived at Eq. (15) from Eq. (7) based on the fact that in our system water was present in a large excess. This model has an ADD% of 6.0%, which is very close to that provided by the power law model. Also the activation energy derived from this model is almost identical to that obtained from the power law model. These indicate that the assumed RDS may be justified. If this is the case, it is because the constraint of requiring two active sites to be available before the reaction can proceed as imposed in this assumption is more stringent as compared with the previous assumption of the adsorption of crude ethanol on an active site. This results in the dissociation of adsorbed crude ethanol taking a much longer time frame as compared with the adsorption of crude ethanol on an active site.

Furthermore, by imposing the values of the constants from Table 4, model 3 reduces to

$$r_A = \frac{k_0 e^{-E/RT} ((N_A N_B^3 / N_C N_D^3) - (N_C N_D^3 / K_P))}{(1 + K_A N_A + (K_Q N_A N_B^2 / N_C N_D^3))} \quad (16)$$

This model has an ADD% of 11%, which makes it reasonable to be included as one of the mechanistic based models. However, a comparison of the activation energies between the power law model and this model shows a significant difference. Based on this large difference, we conclude that the model 3 deviates from the mechanism that is illustrated in the power law model.

The kinetic parameters obtained using the power law model was compared with those obtained by Das [16], in which the collision frequency k_0 and activation energy E are 2.0×10^{-2} and 1.04×10^3 kJ/kmol, respectively. The collision frequencies were well comparable, while the activation energies were different but in the same order of magnitude. The difference in the activation energies could be attributed to the cumulative effects of other organic components in the crude ethanol.

5. Conclusions

The kinetics of crude ethanol reforming over a 15% Ni/Al₂O₃ catalyst has been studied at atmospheric pressure within the temperature range of 596 to 793 K and WHSV within the range of 4.67×10^{-4} – 1.28×10^{-3} s⁻¹. A new kinetic model was proven to describe the experimental kinetics data. This was an Eley Rideal type rate model based on the assumption of dissociative adsorption of crude ethanol on active sites as the rate determining step. The average absolute deviation from the experimental rate is 6%. The model is of the form $-r_A = (2.08 \times 10^3 e^{4430/RT} N_A) / [1 + 3.83 \times 10^7 N_A]^2$. This kinetics model compared excellently with our version of an empirical power law rate model, $-r_A = 3.123 \times 10^{-2} e^{-4410/RT} N_A^{0.43}$ which had an average absolute deviation of 4.5% from the experimental rate.

Acknowledgement

The financial support provided by the Canada Foundation for Innovation (CFI) and HTC Hydrogen Thermochem Corporation, Regina, SK, Canada is gratefully acknowledged.

References

- [1] Cortright RD, Davda RR, Dumesic JA. Hydrogen from catalytic reforming of biomass-derived hydrocarbon in liquid water. *Letts Nat* 2002;418:964–7.
- [2] Haga F, Nakajima T, Yamashita K, Mishima S. Effect of crystallite size on the catalysis of Alumina-supported cobalt catalyst for steam reforming of ethanol. *React Kinetic Catal Lett* 1998;63(2):253–9.
- [3] Creveling HF. Proton exchange membrane (PEM) fuel cell system R & D for transportation applications. In: Proceedings of annual automotive technology development contractors' coordination meeting, Society of automotive engineers. October 19–21, 1992, p. 485–92.
- [4] Dunnison DS, Wilson J. PEM fuel cells: a commercial reality. In: AIAA 29th Intersociety Energy Conversion Engineering Conference. Monterey, CA, 1994. p. 1260–3.
- [5] Whitaker FL. The phosphoric acid PC25™ fuel cell power plant—and beyond. In: AIAA 29th Intersociety Energy Conversion Engineering Conference. Monterey, CA, 1994. p. 1258–9.
- [6] Gary JH, Handwerk GE. Petroleum refining technology and economics. 3rd ed., New York: Marcel Dekker, Inc.; 1994.
- [7] Simanzhenkov V, Idem RO. Crude oil chemistry. New York: Marcel Dekker; 2003.
- [8] Garcia L, French R, Czernik S, Chornet E. Catalytic steam reforming of bio-oils for the production of hydrogen: effects of catalyst composition. *Appl Catal* 2000;201:225–39.
- [9] Cavallaro S, Freni S. Ethanol steam reforming in a molten carbonate fuel cell. A preliminary kinetic investigation. *Int J Hydrogen Energy* 1996;21(6):465–9.
- [10] Athanasio NF, Verykios XE. Reaction network of steam reforming of ethanol over Ni-based catalysts. *J Catal* 2004;225:439–52.
- [11] Athanasios NF, Kondaridesm DI. Production of hydrogen for fuel cells by reformation of biomass-derived ethanol. *Catal Today* 2002;75:145–55.
- [12] Klouz V, Fierro V, Denton P, Katz H, Lisse JP, Bouvot-mauduit S. et al. Ethanol reforming for hydrogen production in a hybrid electric vehicle: process optimization. *J Power Source* 2002;105:26–34.
- [13] Jordi L, Narcis H, Joaquim S, Pilar R. Efficient production of hydrogen over supported cobalt catalysts from ethanol steam reforming. *J Catal* 2002;209:306–17.
- [14] Leclerc S, Mann RF, Peppley BA. Evaluation of the catalytic ethanol-steam reforming process as a source of hydrogen-rich gas for fuel cells. The CANMET Energy Technology Centre (CETC), 1998.
- [15] Galvita VV, Semin GL, Belyaev V, Semikolenov VA, Tsiakaras P, Sobyenin VA. Synthesis gas production by steam reforming of ethanol. *Appl Catal A: General* 2001;220:123–7.
- [16] Das N. Low temperature steam reforming of ethanol. MSc thesis, Department of Chemical Engineering, University of Saskatchewan, Saskatoon, Canada, 2003.
- [17] Idem R, Ibrahim H, Tontiwachwuthikul P, Wilson M. Processing of non-purified ethanol from a glucose fermentation process for solid oxide fuel cell application. In: Gale J, Kaya Y, editors. Proceedings of the sixth international conference on greenhouse gas control technologies. Kyoto, Japan, October 1–4 2002. Oxford, UK: Pergamon; 2003. p. 1825–8.
- [18] Akande A, Idem R, Dalai A. Synthesis, characterisation and performance evaluation of Ni/Al₂O₃ catalysts for reforming of crude ethanol for hydrogen production. *Appl Catal* 2004, submitted.
- [19] Idem RO, Bakhshi NN. Kinetic modeling of the production of hydrogen from methanol-steam reforming process over Mn-promoted coprecipitated Cu–Al catalyst. *Chem Eng Sci* 1996;51(14):3697–708.
- [20] Rase HF. Chemical reactor design for process plants. New York: Wiley; 1987 p. 185–8, 195–9.
- [21] Froment GF, Bischoff KB. Chemical reactor analysis and design. 2nd ed., New York: Wiley Inc.; 1990.
- [22] Geankoplis CJ. Transport processes and separation process principles. Pearson Education, Inc., 2000.
- [23] Visual Numerics Inc. IMSL MATH/LIBRARY: FORTRAN subroutines for mathematical applications. Texas: Visual Numerics Inc.; 1994.
- [24] Ji X, Kritiphat W, Aboudheir A, Tontiwachwuthikul P. Mass transfer parameter estimation using optimization technique: case study in CO₂ absorption with chemical reaction. *Can J Chem Eng* 1999;77:69–73.